Am. J. Hum. Genet. 59:1328–1336, 1996

The Gene for Autosomal Dominant Cerebellar Ataxia Type II Is Located in a 5-cM Region in 3p12-p13: Genetic and Physical Mapping of the SCA7 Locus

G. David,[1] P. Giunti,[2] N. Abbas,[1] P. Coullin,[3] G. Stevanin,[1] W. Horta,[4] R. Gemmill,[5] J. Weissenbach,[6] N. Wood,[2] S. Cunha,[7] H. Drabkin,[5] A. E. Harding,[2,*] Y. Agid,[1] and A. Brice[1]

[1]INSERM U289, Hôpital de la Salpêtrière, Paris; [2]Institute of Neurology, Queen Square, London; [3]INSERM U178, Hôpital Paul Brousse, Villejuif, France; [4]Federal University of Ceara, Hospital Universitario Walter Candido, Forteleza Ce, Brazil; [5]University of Colorado Health Sciences Center, Denver; [6]CNRS URA 1922, Généthon, Evry, France; and [7]Crateus Ceara, Brazil

Summary

Two families with autosomal dominant cerebellar ataxia with pigmentary macular dystrophy (ADCA type II) were investigated. Analysis of 23 parent-child couples demonstrated the existence of marked anticipation, greater in paternal than in maternal transmissions, with earlier age at onset and a more rapid clinical course in successive generations. Clinical analysis revealed the presence of a great variability in age at onset, initial symptom, and associated signs, confirming the characteristic clinical heterogeneity of ADCA type II. The gene for ADCA type II previously was mapped to the spinocerebellar ataxia 7 (SCA7) locus on chromosome 3p12-p21.1. Linkage analysis of the two new families of different geographic origin confirmed the characteristic genetic homogeneity of ADCA type II, distinguishing it from ADCA type I. Haplotype analysis permitted refinement of the SCA7 region to the 5-cM interval between markers D3S1312 and D3S1600 on chromosome 3p12-p13. Eighteen sequence-tagged sites were used for the construction of an integrated map of the candidate region, based on a YACs contig. The entire candidate region is contained in a single nonchimeric YAC of 660 kb. The probable involvement of a CAG trinucleotide expansion, suggested by previous studies, should greatly facilitate the identification of the gene for ADCA type II.

Introduction

The autosomal dominant cerebellar ataxias (ADCAs) are a clinically and genetically heterogeneous group of neurodegenerative disorders. Several neuropathological and clinical classifications have been established (Konigsmark and Weiner 1970; Harding 1982, 1993). In the most commonly and widely accepted classification (Harding 1993), ADCA type II is characterized by progressive cerebellar ataxia associated with pigmentary macular dystrophy. As in other ADCAs, the age at onset, degree of severity, and rate of progression vary among and within families (Benomar et al. 1994). The frequency of associated neurological signs, such as ophthalmoplegia, pyramidal or extrapyramidal signs, deep sensory loss, or dementia, is also variable (Benomar et al. 1994; Enevoldson et al. 1994; Gouw et al. 1994; Martin et al. 1994). As in ADCA type I (Dürr et al. 1993), anticipation is observed and is greater in paternal than in maternal transmissions (Benomar et al. 1994, 1995).

We have previously mapped the gene for ADCA type II, in four families of different geographic origins, to chromosome 3p12-p21.1 (Benomar et al. 1995). Although at least five loci are implicated in ADCA type I (reviewed in Rosenberg 1995), genetic homogeneity is a characteristic of ADCA type II, since two recent studies (Gouw et al. 1995; Holmberg et al. 1995) have reported five other families of various origins linked to this locus, designated "spinocerebellar ataxia 7" (SCA7). The interval for SCA7, deduced from two overlapping candidate regions on chromosome 3p (Benomar et al. 1995; Gouw et al. 1995), had been restricted to ~15 cM between markers D3S1300 and D3S1217.

We report the refinement of the candidate region to 5 cM by linkage analysis and haplotype reconstruction in two new families in which linkage to SCA1, SCA3/MJD, and DRPLA loci had been excluded. Eighteen genetic markers were used to built up a YACs contig that spans this region. The results showed that the SCA7 locus lies within a 660-kb YAC. The large discrepancy between the estimated genetic and physical distances suggests that this region is a possible recombination hot spot.

Subjects and Methods

Families

Two families from Brazil (BRA) and the United Kingdom (UK) were selected for analysis. These were identi-

Received June 20, 1996; accepted for publication September 17, 1996.

Address for correspondence and reprints: Dr. Alexis Brice, INSERM U289, Hôpital de la Salpêtrière, 47 boulevard de l'Hôpital, 75651 Paris CEDEX 13, France. E-mail: brice@u289.ext.infobiogen.fr

*Died on September 11, 1995.

0002-9297/96/5906-0020$02.00

fied during an intensive door-to-door project to detect families with various forms of ADCAs. The two families were classified as ADCA type II, according to the criteria used by Enevoldson et al. (1994). Family BRA originated from a small town in a rural area of northern Brazil. Through a genealogical study back to the late 1700s, we were able to identify the common ancestors of four large branches of the family, providing an eight-generation pedigree with >700 members. Of the 97 affected subjects, 49 were males and 48 were females. Sixty-seven subjects from the two families were examined, including 23 patients.

Clinical Analysis

Age at onset, established by an unsteady gait and/or a visual failure caused by ascertained maculopathy, was determined for 41 patients. Three classes of age were used for comparison of the initial symptom: class I, 0–20 years; class II, 21–40 years; and class III, 41–72 years. Comparisons of means were performed with nonparametric and Student's *t*-tests, and comparisons of frequencies were performed with the χ^2 test or, when necessary, with the Yates corrected χ^2 test.

Genotyping

Blood samples were taken from the 67 consenting individuals, and high-molecular-weight genomic DNA was extracted. Eleven dinucleotide repeats from the Généthon map, placed in the 13 cM between D3S1300 and D3S1285, were selected for the refinement of the SCA7 region (Dib et al. 1996). Genotyping of dinucleotide repeats was determined by PCR amplification, in a final volume of 40 μl, with 100 ng of genomic DNA, 200 μM of each dNTP, and 32 pmol of each primer, in 1 × PCR buffer (500 mM KCl, 70 mM $MgCl_2$, 2 mg BSA/ml, and 160 mM $(NH_4)_2SO_4$). *Taq* DNA polymerase (0.1 unit; ATGC) was added during the first denaturation step (Chou et al. 1992). Then, 35 cycles of denaturation at 94°C for 15 s, annealing at 55°C for 15 s, and extension at 72°C for 15 s were performed, followed by a final extension for 2 min. Aliquots of the PCR products were diluted 1:5 in formamide loading buffer. After a denaturation step at 94°C for 10 min, 2 μl of the mix were loaded on a 6% acrylamide/bis-acrylamide/7 M urea sequencing gel. Then, DNA was blotted on nylon membrane (Hybond N^+; Amersham) and denatured in 0.4 N NaOH for 15 min, and membranes were washed in 2 × SSC. Hybridization was performed at 42°C for 3 h, with a $\gamma^{32}P$ dATP end-labeled $(CA)_{15}$ oligonucleotide in 40 ml of Amasino buffer (Amasino 1986). Membranes were washed at room temperature for 15 min, in 2 × SSC and 0.1% SDS and were exposed overnight to X-ray film.

Linkage Analysis

Pairwise and LOD scores were calculated by use of the MLINK program of the FASTLINK package (version 2.2) (Lathrop and Lalouel 1984; Lathrop et al. 1985; Cottingham et al. 1993; Schäffer et al. 1994). The disease was considered to be autosomal dominant, with a frequency of .0001. Unknown status was attributed to all at-risk individuals who were not clinically examined, as well as to those individuals who were probably affected. Since penetrance of the disease is a function of age, individuals were assigned to the following liability classes determined from the cumulative age-at-onset curve of the analyzed families (data not shown): age 0–9 years, .04; age 10–19 years, .25; age 20–39 years, .57; age 40–59 years, .84; and age >60 years, .98. Because of the weight of as-yet-unaffected at-risk individuals, LOD scores also were calculated by the affected-only method, by setting the penetrance at .001. Allele frequencies for the markers that were used in the linkage analysis were computed from ⩾30 unrelated individuals of different geographic origin. LOD scores also were calculated under the assumption of equal allele frequencies and yielded similar LOD scores (data not shown), indicating true cosegregation and eliminating the possibility that false-positive LOD scores were obtained because of inaccurate allele frequencies. Recombination fractions were assumed to be equal for males and females. The HOMOG program (version 3.10) was used to test genetic homogeneity (Ott 1991).

YAC Contig Formation

Total yeast DNAs from 70 YACs from the CEPH library, previously mapped to chromosome 3p12-p21.1 (Gemmill et al. 1995), were extracted by use of standard protocols. The screening was performed with the 11 polymorphic microsatellite markers from Généthon (Dib et al. 1996) that were used for the genetic analysis and with seven sequence-tagged sites (STSs) derived from either the Whitehead Institute for Biomedical Research database (WI-7177, WI-9056, D3S3119, D3S3395, WI-8051, and D3S3068) or the Cooperative Human Linkage Center database (GATA-61E08). PCR was performed by use of the same procedures as described previously. For each PCR set, a positive (human genomic DNA) and a negative (pyrolysed water) control were added to ascertain the absence of contaminant. Aliquots of the PCR products were mixed 5:1 with loading buffer (0.05% bromophenol and 60% glycerol) and were run on a 1% agarose gel containing 0.5 μg of ethidium bromide/ml. To avoid false-negative YACs, PCR were performed at least twice for each DNA.

FISH

Chromosomal analysis of the chimerism of the 11 YACs was performed by FISH according to a protocol described elsewhere (Rosier et al. 1994; Goguel et al., in press). Probes were obtained by PCR amplification of the human YAC insert, with *Alu* S (5′ GCCACTG-CACTCCAGCCTGGG 3′) and *Alu* R (5′ GCCTC-

CCAACGTGCTGGATTACAG 3′) primers. An annealing temperature of 55°C was chosen, with both primers combined in the same PCR, and 30% of labeled nucleotide (biotin-16-dUTP) was used and incorporated into the reaction. Since repetitive elements also are amplified in these PCR conditions, a competition using human placenta and human Cot-1 DNA was required for the suppression of the fluorescent *Alu* background. Hybridizations were performed on human metaphase spreads prepared from phytohemagglutinin-stimulated lymphocytes obtained from healthy donors. They were examined with a Leica Aristoplan microscope equipped with epifluorescence. Microphotographs were taken by use of an oil-immersion objective 100× and the Leica MPS46 automatic system.

Results

Clinical Evaluation and Anticipation Analysis

Mean age at onset, 32 ± 17 years (range 1–72 years), was similar in families BRA and UK, and mean disease duration was 16 ± 10 years (range 1–29 years). Clinical information was collected from 41 patients from family BRA, to determine the first symptom of the disease. The sex of the transmitting parent also was ascertained for 36 patients. When the disease was transmitted by the mother ($N = 13$), it started, in 54% of the subjects, with visual failure; in 38%, with ataxia; and, in 8%, with ataxia and visual failure. In the offspring of an affected father ($N = 23$), in only 22% did the disease start with visual failure, and in the other 78% it started equally with ataxia or ataxia together with visual failure. Although the difference was not quite statistically significant ($P = .06$), this suggests that the sex of the transmitting parent influenced the nature of the first symptom. Age at onset also influenced the initial symptom. We did not find a significant difference between classes I and II, but in class III the disease started with ataxia in 7 of 10 patients, and in the remaining 3 it started with ataxia and visual failure at the same time; but in none did it start with visual failure alone ($P < .03$). All the subjects who initially had isolated maculopathy ($N = 12$) developed an ataxic gait after a variable period of time (1–22 years). Most of the subjects in whom the disease started with ataxia ($N = 14$) developed visual failure after 1–21 years, except for two subjects, ages 53 and 80 years, in whom visual failure was absent after 5 and 8 years of evolution, respectively.

The clinical features of 23 examined patients are summarized in table 1. Eighteen of 23 patients showed various degrees of ophthalmoplegia. In the very early stage of the disease, gaze restriction was supranuclear, but it became nuclear as the disease evolved. Computed-tomography (CT) scans were performed in one patient from each family and showed cerebellar and brain-stem atrophy. Eighteen patients were wheelchair bound after a mean duration of 12 ± 6 years. Patients BRA-8993, BRA-9015, and UK-9178 had no affected first-degree relatives, but, on neurological examination, they showed clear signs of the same disease that affected other family members. Patient BRA-8993, age 48 years, presented with a 10-year history of bilateral visual failure and 5 years of unsteadiness. At examination, an ataxic gait was evident, with moderate limb ataxia and dysarthria. Marked restriction of upgaze and lateral gaze was present, as well as slowing of saccades in all directions. Tendon reflexes were pathologically brisk, and plantar reflexes were unresponsive. There were no extrapyramidal signs; power, tone, and sensation were normal. Fundoscopy showed the absence of a macular reflex and mottling of pigment at the macula in both eyes. Her father had died of cancer at age 47 years, without any neurological symptoms or signs. Patient BRA-9015, seen at the age of 53 years, had at that time a 5-year history of unsteady gait. None of her two offspring and none of her five siblings showed signs of the disease. After 5 years of evolution, she presented with moderate ataxia of gait and dysmetria, dysarthria, downbeat nystagmus, upgaze ophthalmoplegia, brisk reflexes, and impassive facies. She did not complain of decreased visual acuity, and maculopathy was absent on fundoscopy. Her father died of a heart attack at the age of 60 years. According to the family informant, the father had diabetes and a >10-year history of progressive leg "weakness." A few years before his death he had developed bilateral ptosis and visual failure, especially of central vision. This suggests that he was affected with the same disease as his daughter. Patient UK-9178 presented at the age of 14 mo, with unsteadiness. By age 17 mo she was unable to sit or stand without support. Intentional tremor was evident in the hands, and there was positional tremor of the head. Dysphagia, slightly increased tendon reflexes, and increased macular

Table 1

Clinical Features of 23 Patients with ADCA Type II

	Family BRA	Family UK
No. of patients	21	2
Mean age at onset (years)	32 ± 14	40 ± 55
Disease duration (years)	13 ± 8	8 ± 9
Truncal ataxia	21/21	2/2
Visual failure	17/21	1/2
Limb ataxia	19/21	2/2
Dysarthria	20/21	2/2
Nystagmus	9/21	0/2
Ophthalmoplegia	17/21	1/2
Slow saccades	8/21	0/2
Dysphagia	10/21	1/2
Pyramidal signs	21/21	1/2
Chorea	1/21	0/2
Dystonia	2/21	0/2
Sensory loss	3/21	0/2
Dementia	0/21	1/2

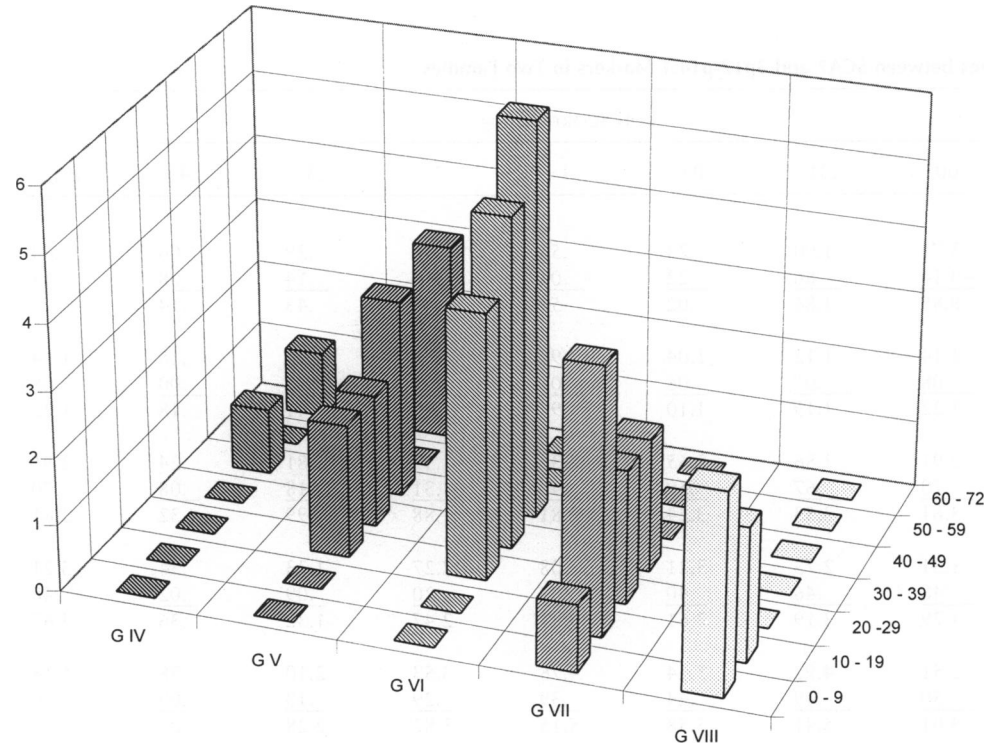

Figure 1 Distribution of age at onset for 41 patients from family BRA, according to generation. Anticipation is shown by the younger age at onset in successive generations.

pigmentation were observed. A marked hypotonia was present. At this stage she already showed clear mental deterioration. A CT scan performed at the time revealed cerebellar and brain-stem atrophy. Her father, in his mid 40s, is still asymptomatic.

In family BRA, the mean age at onset decreased from generation to generation: generation IV, 50 ± 14 years, $N = 2$; generation V, 45 ± 16 years, $N = 10$; generation VI, 35 ± 9 years, $N = 16$; generation VII, 17 ± 9 years, $N = 8$; and generation VIII, 7 ± 7 years, $N = 5$ ($P < .002$). The distribution according to the generations is shown in figure 1. Disease duration until death also decreased: generation IV, 29 ± 13 years, $N = 2$; generation V, 17 ± 6 years, $N = 6$; generation VI, 20 ± 2 years, $N = 2$; generation VII, 7 ± 7 years, $N = 2$; and generation VIII, 2 ± 0 years, $N = 3$ ($P < .05$). The decreasing age at onset in successive generations is associated with a decreasing disease duration, which reflects a more severe course of the disease. The sex of the affected parent influenced anticipation, which was greater in paternal (22.8 ± 13.3 years, $N = 15$) than in maternal transmissions (12.5 ± 6.2 years, $N = 8$) ($P < .02$). The age at onset was influenced neither by the sex of the affected subjects nor by the sex of the transmitting parents. However, four of the five affected children had the disease transmitted by their father, one by its mother. In the five affected children, four from family BRA and one from family UK, the disease started between 8 mo and 2 years of age, and all five died before age 5 years. There was a positive correlation between the age at onset and disease duration to death (mean 15.1 ± 10 years, $N = 15$, $P < .0005$), indicating the presence of true anticipation. Finally, incomplete penetrance was suggested by the observation of six apparently unaffected subjects at the time of death, three females and three males, who had transmitted the disease to at least one offspring. Three of the obligate carriers died before the age of 50 years, and the remaining three died at ages 52, 65, and 70 years.

Linkage Analysis

Pairwise linkage analysis in the Brazilian family BRA generated significant LOD scores of 3.21 at $\theta = .06$, 5.18 at $\theta = .04$, and 3.44 at $\theta = .00$ for markers D3S1600, D3S1287, and D3S3635, respectively (table 2). For marker D3S3698, a maximum LOD score (Z_{max}) of 2.91 was obtained at $\theta = .00$. In the British family UK, positive values of .70 at $\theta = .00$, .48 at $\theta = .00$, and .50 at $\theta = .00$ for markers D3S3698, D3S1600, and D3S1287, respectively, were suggestive of linkage. A test for linkage homogeneity was performed for marker D3S1600, with families BRA and UK and with the four families CA-1, RBT-002, RBT-007, and SAL-313 analyzed in a previous study (Benomar et al. 1995). With the HOMOG program (Ott 1991), the hypothesis of linkage and genetic homogeneity was supported with odds of 7

Table 2

Pairwise LOD Scores between SCA7 and 3p12-p14.1 Markers in Two Families

Marker and Family	LOD Score at θ = .00	.01	.05	.1	.2	.3	.4	Z_{max}	Maximum θ
D3S1312:									
BRA	−5.74	−1.00	.24	.58	.56	.29	.06	.64	.14
UK	−3.14	−.86	−.22	.01	.14	.14	.08	.15	.24
Overall	−8.88	−1.86	.02	.59	.70	.43	.14	.70	.20
D3S3566:									
BRA	1.14	1.12	1.04	.92	.66	.40	.18	1.14	.00
UK	.08	.07	.06	.05	.03	.01	.00	.08	.00
Overall	1.22	1.19	1.10	.97	.69	.41	.18	1.22	.00
D3S3698:									
BRA	2.91	2.86	2.65	2.33	1.57	.81	.24	2.91	.00
UK	.70	.67	.59	.48	.31	.18	.08	.70	.00
Overall	3.61	3.53	3.24	2.81	1.88	.99	.32	3.61	.00
D3S1600:									
BRA	1.31	2.73	3.21	3.08	2.27	1.23	.34	3.21	.05
UK	.48	.46	.40	.33	.20	.09	.02	.48	.00
Overall	1.79	3.19	3.61	3.41	2.47	1.32	.36	3.67	.07
D3S1287:									
BRA	2.51	4.92	5.14	4.76	3.53	2.10	.78	5.18	.04
UK	.50	.49	.44	.39	.29	.18	.09	.50	.00
Overall	3.01	5.41	5.58	5.15	3.82	2.28	.87	5.75	.07
D3S3635:									
BRA	3.44	3.36	3.04	2.62	1.75	.89	.22	3.44	.00
UK	−3.67	−1.28	−.61	−.35	−.13	−.04	−.01	.00	.50
Overall	−.23	2.08	2.43	2.27	1.62	.85	.21	2.44	.12

$\times 10^7$ against the hypothesis of no linkage. Posterior probabilities of linkage with D3S1600 were 1.00, .72, 1.00, .75, .83, and .66 for families BRA, UK, CA-1, RBT-002, RBT-007, and SAL-313, respectively.

Calculations also were performed with the more conservative "affected-only" method and showed, in family BRA, significant values of 3.29 at θ = .04, 3.59 at θ = .00, and 4.36 at θ = .03 for markers D3S3631, D3S3698, and D3S1287, respectively (data not shown). For marker D3S3698, the higher Z_{max} in the affected-only calculation probably was due to the frequency of the linked allele (40%), present in many asymptomatic "at-risk" individuals. In family UK, pairwise LOD scores gave similar results (data not shown).

Recombination events, detected by haplotype reconstruction, confirmed the results obtained by linkage analysis. Interestingly, the three patients with no affected first-degree relatives carried the haplotype segregating with the disease in their family (BRA-8993 [data not shown] and UK-9178) or part of it (BRA-9015). The telomeric boundary was defined by the independent recombination events observed in individuals BRA-9023, BRA-9015, and UK-8053 (fig. 2), between the SCA7 locus and marker D3S1312. A single recombination event between the SCA7 locus and marker D3S1600, in individual BRA-9015, defined the centromeric boundary (fig. 2). This recombination event must have occurred in an older generation, since the recombinant haplotype linked to the disease in individual BRA-9015 is carried also by three of her siblings. This result is in accordance with the recombination event, observed in still-unaffected individual UK-9176 and transmitted to her affected daughter UK-9178, between marker D3S3635 and the disease locus. The SCA7 locus thus can be restricted to the 5-cM interval between markers D3S1312 and D3S1600.

Physical Mapping of the SCA7 Locus: YAC Contig Construction

DNA from the 70 selected YACs was screened for 18 genetic markers that span 13 cM between D3S1300 and D3S1285. These markers failed to identify 19 YACs, which were eliminated from the study. Comparison of marker content among YACs permitted us to estimate their overlap and to order them along the genetic map (summarized in fig. 3). The order of the genetic markers from the Généthon map (Dib et al. 1996) was confirmed, except for marker D3S3631. This marker, which was found to map between D3S1300 and D3S1312, previously had been placed at the same locus as D3S3566 on the Généthon map. Similarly, we were able to order other markers—D3S3635, D3S3571, and D3S3644—placed at the same locus. These results were confirmed by the observation of recombination events either be-

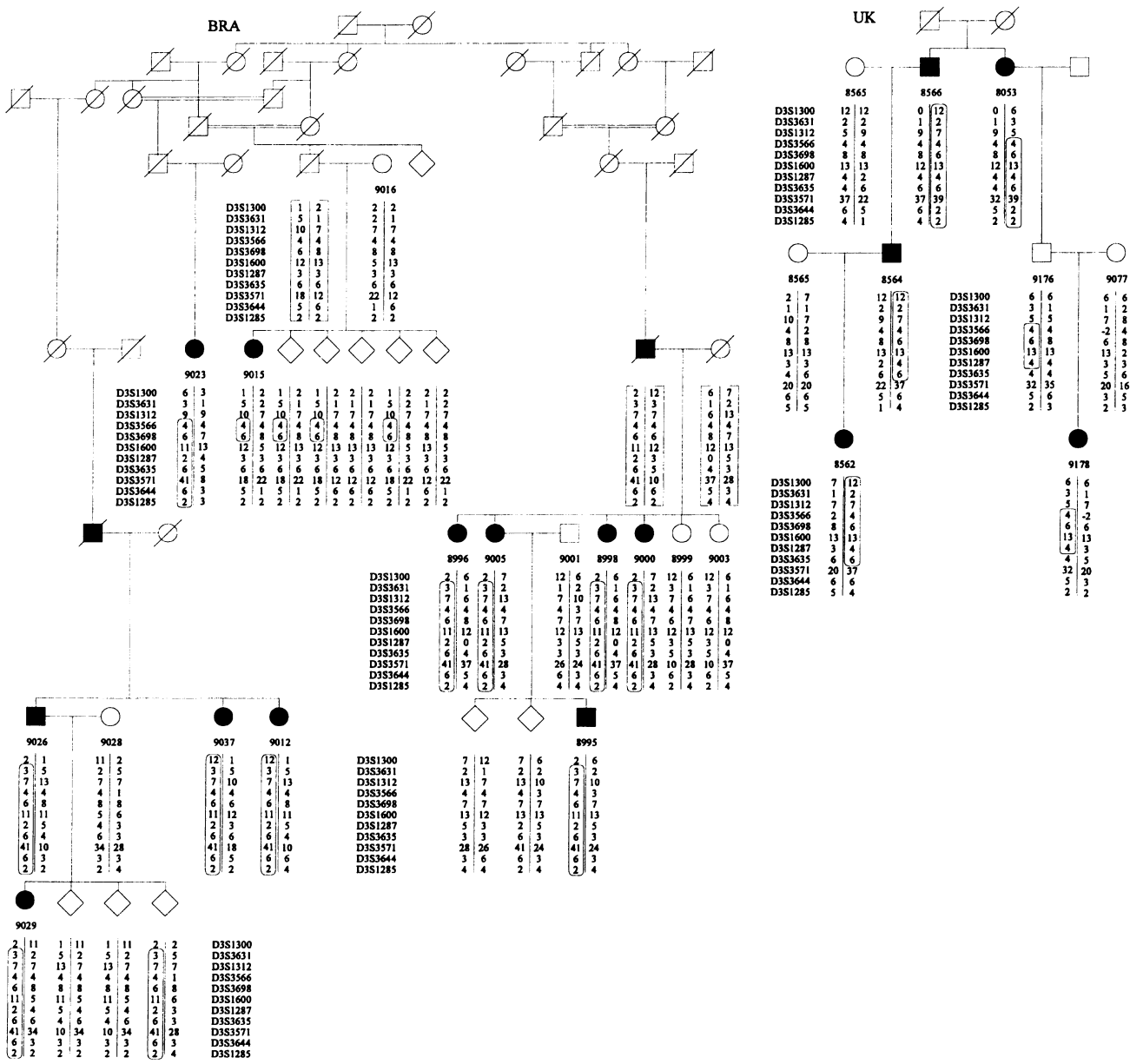

Figure 2 Haplotype reconstruction in partial pedigrees of two families presenting with ADCA type II. Reconstructed haplotypes for 11 chromosome 3p microsatellite markers are represented below the symbols. Haplotypes segregating with the disease are boxed. Deduced haplotypes are bracketed.

tween markers D3S3631 and D3S1312 in a family described elsewhere (Benomar et al. 1995) or between markers D3S3635 and D3S3571 in family UK (fig. 2). Nonpolymorphic markers were ordered on the framework map determined with the polymorphic microsatellites. All orders are supported by the information generated by at least two YACs.

FISH Analysis

Eleven YACs (801__a__8, 830__a__12, 882__d__9, 910__d__16, 924__b__12, 965__a__3, 846__g__11, 953__a__12, 842__e__6, 811__f__12, and 823__f__12) were selected for a minimal contig of the SCA7 locus, according to their large size and marker content. All these YACs were tested for chimerism, by FISH. All YACs except 965__a__3 yielded specific signal on chromosome 3p12-p13. Chimerism was detected for three YACs: 882__d__9, 910__d__6, and 811__f__12. Two nonchimeric YACs, 830__a__12 (660 kb) and 801__a 8 (1,520 kb), contained all the STSs between D3S1312 and D3S1600, which define the boundaries of the candidate interval.

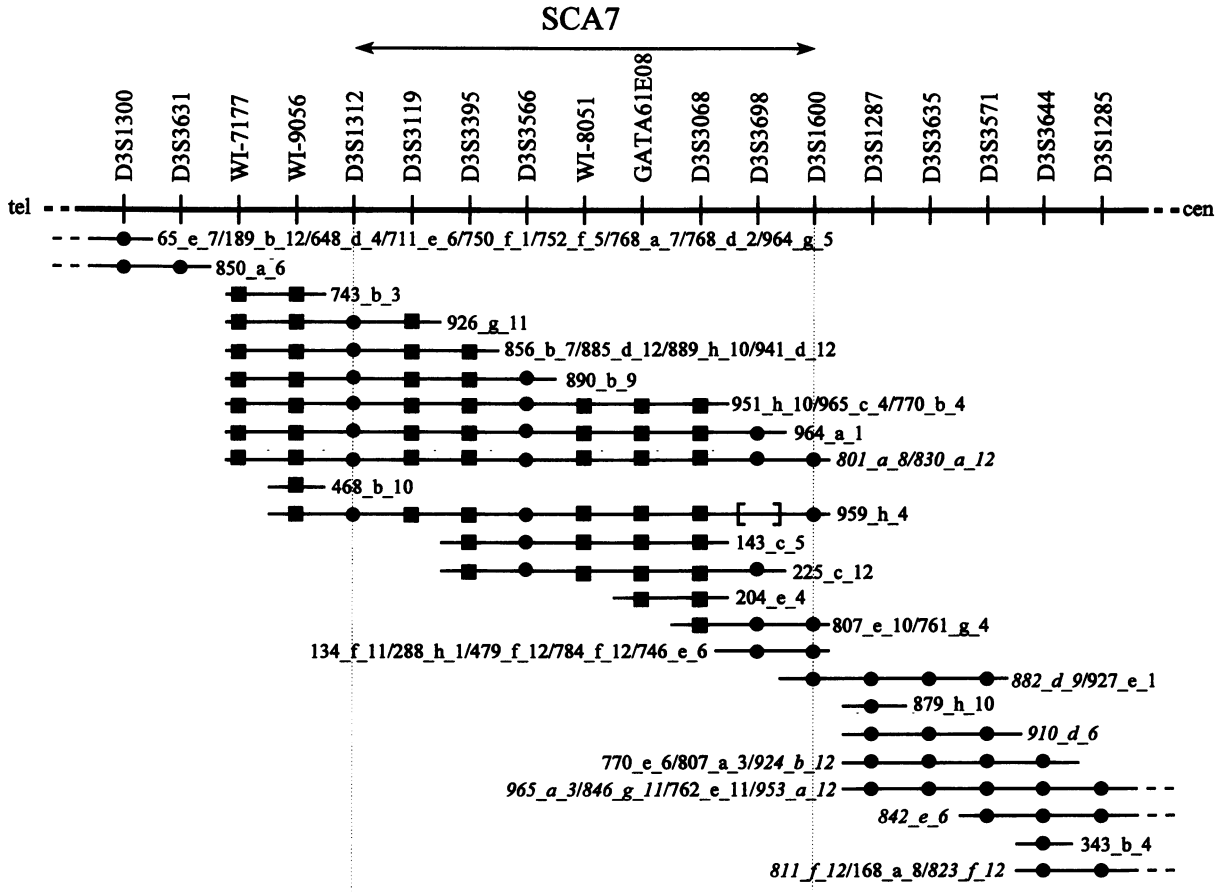

Figure 3 Contig map spanning the SCA7 locus on chromosome 3p12-p13. The SCA7 candidate region is defined by dotted lines. Polymorphic markers are represented by black circles, and nonpolymorphic markers are represented by black squares. Deletions are represented by brackets, and YACs tested by FISH are in italics.

Discussion

In this study, linkage and haplotype analyses of two new families originating from Brazil and the United Kingdom reduced the SCA7 region to the 5-cM interval between the markers D3S1312 and D3S1600, on chromosome 3p12-p13. This interval is covered entirely by a nonchimeric 660-kb YAC.

ADCA type II is clinically distinct from the other ADCAs. The great variability in age at onset, initial symptom, disease duration, and age at death are the main characteristics. As opposed to the situation in childhood- or young-adult-onset cases, loss of vision is not observed as the initial symptom in late-onset patients. This could be explained by the physiological decline that may overshadow the pathological sign, the more benign course of the disease in this age class, and/or the fact that the lesion may remain infraclinical for many years (Benomar et al. 1994; Enevoldson et al. 1994). Detailed color-vision analyses, particularly for the blue/yellow axis, should have been useful in detecting early maculopathy, but, unfortunately, it was not possible to include them in the evaluation protocol used in the present study. Our results agree with other reports, confirming anticipation that is greater in paternal than in maternal transmissions, with earlier age at onset and with a more rapid clinical course in successive generations (Benomar et al. 1994, 1995). The effect of parental sex is evident in severe infantile forms, which were paternally transmitted in four of five cases. Anticipation could also account for some cases of incomplete penetrance. Six asymptomatic individuals with various ages at death and/or examination, $\leq$72 years of age, were obligate gene carriers, as attested by the observation of an affected child. The parental sex also could affect the nature of the first symptom of the disease, as reported for other disorders caused by unstable trinucleotide repeats—disorders such as Huntington disease, in which subjects with the rigid form have a preponderance of affected fathers (Harper 1991).

Linkage analysis with 11 microsatellite markers established that SCA7 is the locus for ADCA type II in two new families from the United Kingdom and Brazil. Taken together with previous analyses of families of various geographical origins, these results strongly support the hypothesis that ADCA type II, unlike ADCA

type I (Rosenberg 1995), constitutes a single genetic entity (Benomar et al. 1995; Gouw et al. 1995; Holmberg et al. 1995). Haplotype reconstruction revealed, in patients, independent recombination events that defined the telomeric boundary. The centromeric boundary was defined by the single recombination event between marker D3S1600 and the disease locus detected in patient BRA-9015, age 53 years, also observed in three still-asymptomatic siblings. This patient presented with typical cerebellar ataxia associated with ophthalmoplegia and brisk reflexes but with no loss of visual acuity, which can manifest much later than the cerebellar syndrome, especially in late-onset cases (Benomar et al. 1994).

The refinement of the SCA7 region permitted the construction of a physical map based on a YAC contig. Eighteen polymorphic or STS markers were placed on this map, in an order that minimized YAC deletions. The order of the polymorphic markers at different loci was identical on the Généthon genetic map and the YAC contig, except for marker D3S3631. For this marker and those placed at the same locus, the order on the physical map was confirmed by recombination events observed in SCA7 families. Finally, the order of the other STSs, based on the information from at least two YACs, still must be confirmed.

Most of the resulting map is consistent with previous reports (Whitehead Institute for Biomedical Research database; Gemmill et al. 1995). However, three YACs—143__c__5, 204__e__4, and 225__c__12—were mapped to an interval different than that described by Gemmill et al. (1995). In the latter map, all these YACs were deleted for probe D3S2589, generated by the YAC 340F6L end, suggesting that this probe does not map to the interval between D3S311 and D3S2598. We propose that markers between D3S311 and D3S2598 should be positioned between D3S1312 and D3S316. This order reduces the number of deletions in nine YACs but creates deletions in only two YACs, 413__c__6 and 134__f__11.

Two nonchimeric YACs, 801__a__8 and 830__a__12, carry all the STSs that span the candidate region. If YAC 830__a__12 is not deleted, the SCA7 candidate region is <660 kb. According to the usual estimate of 1 cM for 1 Mb, the recombination rate in this 660-kb region is approximately eightfold greater than expected. This suggests that the SCA7 region might be a recombination hot spot.

An unstable translated $(CAG)_n$-triplet expansion has been implicated in five other neurodegenerative disorders, including two subtypes of autosomal dominant cerebellar ataxia (La Spada et al. 1991; The Huntington's Collaborative Research Group 1993; Orr et al. 1993; Kawaguchi et al. 1994; Koide et al. 1994; Nagafuchi et al. 1994). We confirm that, as in these disorders, anticipation is a major characteristic in ADCA type II. A recent study has established that an expanded polyglutamine tract, encoded either by a $(CAG)_n$ expansion or by a $(CAA)_n$ expansion, is implicated in ADCA type II (Trottier et al. 1995). Furthermore, repeat-expansion detection (RED) assays (Shalling et al. 1993) suggest that expanded CAG repeats cosegregate with the disease (Linblad et al., in press). Taken together, the knowledge of the probable involvement of a CAG repeat and the refinement of the SCA7 locus to a 660-kb interval, entirely covered by a YAC contig, should facilitate identification of the responsible gene.

Acknowledgments

This work is dedicated to Prof. A. E. Harding. We thank M. Ruberg for critical reading of the manuscript, and we thank C. Scarpelli, P. Gesnouin, and C. Hascoet, all at Infobiogen (Villejuif, France), for their help with the linkage calculations. We also thank D. Le Paslier at CEPH for providing the YACs. The support of Généthon, particularly of S. Fauré, is gratefully acknowledged. We especially thank the families for their participation in this study. We are also grateful to the Association Française contre les Myopathies, the VERUM Foundation, the Groupement d'Etudes et de Recherches sur les Génomes, the Association pour le Développement de la Recherche sur les Maladies Génétiques Neurologiques et Psychiatriques, and the Biomed Concerted Action (grant 708039 CEE BRICE). R.G. and H.D. are supported by NIH grant R01 HG000358.

References

Amasino RM (1986) Acceleration of nucleic acid hybridization rate by polyethylene glycol. Ann Biochem 152:304–307

Benomar A, Krols L, Stevanin G, Cancel G, Le Guern E, David G, Ouhabi H, et al (1995) The gene for autosomal dominant cerebellar ataxia with pigmentary macular dystrophy maps to chromosome 3p12-p21.1. Nat Genet 10:84–88

Benomar A, Le Guern E, Dürr A, Ouhabi H, Stevanin G, Yahyaoui M, Chkili T, et al (1994) Autosomal-dominant cerebellar ataxia with retinal degeneration (ADCA type II) is genetically different from ADCA type I. Ann Neurol 35: 439–444

Chou Q, Russel M, Birch DE, Raymond J, Bloch W (1992) Prevention of pre-PCR mis-priming and primer dimerization improves low-copy-number amplifications. Nucleic Acids Res 20:1717–1723

Cottingham RW Jr, Idury RM, Schäffer AA (1993) Faster sequential genetic linkage computations. Am J Hum Genet 53:252–263

Dib C, Fauré S, Fizames C, Samson D, Drouot N, Vignal A, Millasseau P, et al (1996) A comprehensive genetic map of the human genome based on 5,264 microsatellites. Nature 380:152–154

Dürr A, Chneiweiss H, Khati C, Stevanin G, Cancel G, Feingold J, Agid Y, et al (1993) Phenotypic variability in autosomal dominant cerebellar ataxia type I is unrelated to genetic heterogeneity. Brain 116:1497–1508

Enevoldson TP, Sanders MD, Harding AE (1994) Autosomal

dominant cerebellar ataxia with pigmentary macular dystrophy: a clinical and genetic study of eight families. Brain 117: 445–460

Gemmill RM, Chumakov I, Scott P, Waggoner B, Rigault P, Cypser J, Chen Q, et al (1995) A second-generation YAC contig map of human chromosome 3. Nature Suppl 377: 299–319

Goguel AF, Pulcini F, Danglot G, Fauvet D, Devignes MD, Bernheim A. Mapping of 22 YACs on human chromosomes by FISH using yeast DNA Alu-PCR products for competition. Ann Genet (in press)

Gouw LG, Digre B, Harris CP, Haines JH, Ptacek LJ (1994) Autosomal dominant cerebellar ataxia with retinal degeneration: clinical, neuropathologic, and genetic analysis of a large kindred. Neurology 44:1441–1447

Gouw LG, Kaplan CD, Haines JH, Digre B, Rutledge SL, Matilla A, Leppert M, et al (1995) Retinal degeneration characterizes a spinocerebellar ataxia mapping to chromosome 3p. Nat Genet 10:89–93

Harding AE (1982) The clinical features and classification of the late onset autosomal dominant cerebellar ataxias. Brain 105:1–28

——— (1993) Clinical features and classification of inherited ataxias. In: Harding AE, Deufel T (eds) Advances in neurology. Vol 61: Inherited ataxias. Raven, New York, pp 1–14

Harper PS (1991) Genetic aspects of Huntington's disease. In: Harper PS (ed) Huntington's disease. WB Saunders, London, pp 281–318

Holmberg M, Johansson J, Forsgren J, Heijbel J, Sandgren O, Holmgren G (1995) Localization of autosomal dominant cerebellar ataxia associated with retinal degeneration and anticipation to chromosome 3p12-p21.1. Hum Mol Genet 4:1441–1445

Huntington's Disease Collaborative Research Group, The (1993) A novel gene containing a trinucleotide repeat that is expanded and unstable on Huntington's disease chromosomes. Cell 72:971–983

Kawaguchi Y, Okamoto T, Taniwaki M, Aizawa M, Inoue M, Katayama S, Kawakami H, et al (1994) CAG expansions in a novel gene for Machado-Joseph disease at chromosome 14q32.1. Nat Genet 8:221–228

Koide R, Ikeuchi T, Onodera O, Tanaka H, Igarashi S, Endo K, Takahashi H, et al (1994) Unstable expansion of a CAG repeat in hereditary dentatorubral-pallidoluysian atrophy (DRPLA). Nat Genet 6:9–13

Konigsmark BW, Weiner LP (1970) The olivo-ponto-cerebellar atrophies: a review. Medicine 49:227–242

Lathrop GM, Lalouel JM (1984) Easy calculations of lod scores and genetic risks on small computers. Am J Hum Genet 36:460–465

Lathrop GM, Lalouel JM, Julier C, Ott J (1985) Multilocus linkage analysis in humans: detection of linkage and estimation of recombination. Am J Hum Genet 37:482–498

La Spada AR, Wilson EM, Lubahn DB, Harding AE, Fischbeck KH (1991) Androgen receptor gene mutations in X-linked spinal and bulbar muscular atrophy. Nature 352:77–79

Lindblad K, Savontaus ML, Stevanin G, Holmberg M, Digre K, Zander C, Ehrsson H, et al. An expanded CAG repeat sequence in spinocerebellar ataxia 7. Genome Res (in press)

Martin J-J, Van Regemorter N, Krols L, Brucher J-M, de Barsy T, Szliwowski H, Evrard P, et al (1994) On an autosomal dominant form of retinal-cerebellar degeneration: an autopsy study of five patients in one family. Acta Neuropathol 88:277–286

Nagafuchi S, Yanagisawa H, Sato K, Shirayama T, Ohsaki E, Bundo M, Takeda T, et al (1994) Dentatorubral and pallidoluysian atrophy expansion of an unstable CAG trinucleotide on chromosome 12p. Nat Genet 6:14–18

Orr HT, Chung M-Y, Banfi S, Kwiatkowski TJ Jr, Servadio A, Beaudet AL, McCall AE (1993) Expansion of an unstable trinucleotide CAG repeat in spinocerebellar ataxia type 1. Nat Genet 4:221–226

Ott J (ed) (1991) Analysis of human genetic linkage, 2d ed. John Hopkins University Press, Baltimore

Rosenberg RN (1995) Autosomal dominant cerebellar phenotypes: the genotype has settled the issue. Neurology 45:1–5

Rosier MF, Goguel AF, Martin A, Le Paslier D, Coullin P, Houlgatte R, Bernheim A, et al (1994) A 1.7 Mb contig around the human BDNF gene (11p13): integration of the physical, genetic, and cytogenetic maps in relation to WAGR syndrome. Genomics 24:69–77

Schäffer AA, Gupta SK, Shriram K, Cottingham RW Jr (1994) Avoiding recomputation in genetic linkage analysis. Hum Hered 44:225–237

Schalling M, Hudson TJ, Buetow KH, Houseman DE (1993) Direct detection of novel expanded trinucleotide repeats in the human genome. Nat Genet 4:135–139

Trottier Y, Lutz Y, Stevanin G, Imbert G, Devys D, Cancel G, Saudou F, et al (1995) Polyglutamine expansion as a pathological epitope in Huntington's disease and four dominant cerebellar ataxias. Nature 378:403–406

Whitehead Institute for Biomedical Research. http://www.genome.wi.mit.edu